Single Image Dehazing Using Fixed Points and Nearest-Neighbor Regularization

Shengdong Zhang and Jian Yao[✉]

Computer Vision and Remote Sensing (CVRS) Lab,
School of Remote Sensing and Information Engineering, Wuhan University,
Wuhan, Hubei, People's Republic of China
jian.yao@whu.edu.cn
http://cvrs.whu.edu.cn/

Abstract. Natural images captured in bad weather conditions often suffer from poor visibility. Dehazing, the process of removing haze from a single input image or multiple images, is a crucial task in image and video processing, which is quite challenging because the number of freedoms is lager than the number of observations. In this paper, we propose a novel method to reduce the block artifacts and halos for single image dehazing, which replaces the widely used soft matting and contextual regularization. We first find some fixed points in a maximum filter and then apply a Nearest-Neighbor (NN) regularization to recover a smooth transmission map. Compared with the state-of-the-art single image dehazing methods, the experimental results on some typical and challenged images demonstrate that our method can produce a high-quality dehazed image and recover the fine detail information and vivid color from the image haze regions.

1 Introduction

Natural images captured in outdoor scenes are often suffered by bad weather conditions such as air particles, water droplets, fog, haze, smoke, rain or snow. In such cases, atmospheric phenomena such as haze and fog caused by atmospheric absorption and scattering will greatly reduce the visibility and quality of the images captured in the scenes. The light received by camera sensors from the object in the scene is attenuated along the light propagating direction. The arriving light is fused with the air-light [1] - the ambient light reflected into the line of sight by air particles. Vividness, visibility and contrast of a natural image captured in outdoor under these bad weather conditions are dramatically degraded, which make it hard to recognize the objects existed in this image farther away from the camera center. As shown in Fig. 1(a), the degraded image loses color fidelity and contrast and the distant objects in the image are hard to be distinguished. As stated in [2], the degradation is spatially variant because the scattering depends on the distance between the camera and the objects existed in the scene.

Restoring images captured in outdoor under the bad weather conditions has caused great interesting in the past decade. Haze removal is quite needed in
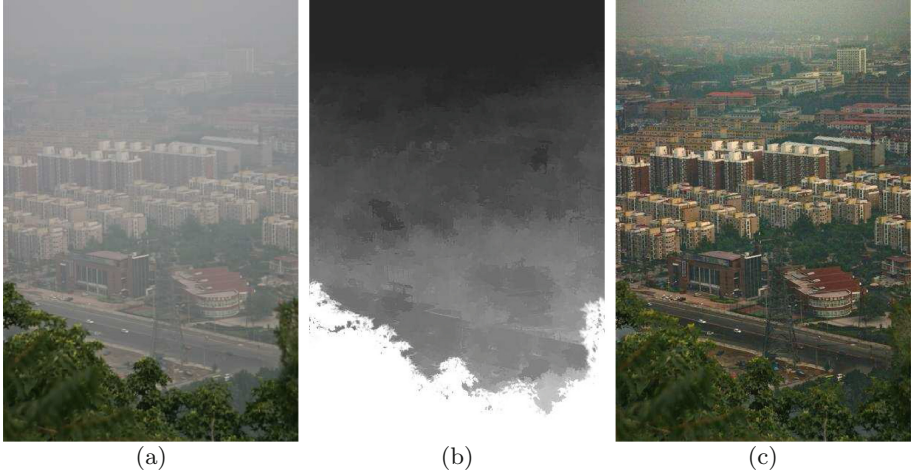
Fig. 1. An illustration example for our proposed single image dehazing approach: (a) The input hazy image; (b) Our recovered transmission map; (c) The dehazed image. (Color figure online)

computer vision applications and commercial/computational photography. First, removing haze can improve the visibility of the image and correct the color distortion caused by the air-light. In general, the haze-free image is more visual friendly. Second, most computer vision algorithms, such as feature detection, filtering and image analysis, usually assume that the input image is haze-free. The performance of computer vision algorithms and advanced image editing ones will be greatly degraded by the low contrast and visibility images. Last, bad weather conditions will cause traffic accidents due to the poor visibility. If the haze removing techniques can be efficiently utilized for the car navigation, the image visibility can be greatly improved and the traffic accidents are possibly reduced to some extent. However, defogging or haze removal is a very challenging because the amount of scattering depends on the unknown distances of the camera and the scene points and the air-light is also unknown. Obviously, this is a quite ill-posed problem especially when the input is only a single hazy image. Therefore, those early proposed methods for haze removal rely on multiple images of the same scene and the additional depth information [3–5]. For example, in [3], the depth discontinuities in the scene and scene structure were computed by using the changes in intensities of scene points under different weather conditions. In [4,6], the polarization based methods were proposed to remove image haze through two images taken with different degrees of polarization. Kopf et al. [5] developed a depth-based method to dehaze an image by using the scene depth information, which are directly accessible in the geo-referenced digital terrain or city models. Although all these methods can produce good results, but the constrain on input limits the applications of these methods.

Recently, removing haze from a single image attracted much attention and made significant progresses due to its wide applications. A lot of single image haze removal methods have been proposed based on the assumption or stronger priors. Comparing haze-free images and haze ones, Tan [7] found that the haze-free images have high contrast than the haze ones. Based on this observation, he proposed an interesting single image haze removal method by maximizing the local contrast of the restored image. This method can yield a visually compelling results. However, the restored image often exists color shift, block artifacts and significant halos because this method might not be physically valid. Fattal [8] proposed to remove haze from a color image under the assumption that the surface texture and the transmission are locally uncorrelated, which is used to solve the air-light-albedo ambiguity. This method is physical sound and can yield compelling results. However, it is time-consuming and cannot deal with the grayscale images. In addition, it could fail to deal with dense-hazy images. Fattal [9] proposed another method for single-image dehazing, which relies on pixels of small patches in natural images, which often show a one-dimensional distribution in the RGB color space. In this method, a local model was proposed to explain the color-lines in the context of hazy scenes and recovering the scene transmission by considering the lines' offset from the origin. A new Markov random field was described for yielding complete and regularized transmission.

He et al. [2] proposed a novel dark channel prior based dehazing method, which is a basis of the dark-object subtraction methods [10]. The dark channel prior means that in most local patches there exists often at least one color (RGB) channel containing some pixels with very low intensities. With this prior, He et al. estimated the thickness of haze locally from the dark-channel pixels found within a local patch. This method is very simple, physically sound and can produce impressive results even in images with heavy haze. However, it cannot deal with the sky images quite well because the dark channel pixels are possibly unavailable in those bright image regions. In addition, it is time-consuming. Recently, a lot of methods have been proposed to overcome the weakness of the Dark Channel Prior (DCP). For example, He et al. [11], Tarel and Hautiere [12] and Tarel et al. [13] used "median of median filter" and guided filtering to replace soft matting. Carr and Hartley [14] combined the scene geometry and the dark channel prior to estimate the transmission, and used the alpha-expansion optimization technique to recover a smooth transmission map. Gibson and Nguyen [15] proposed a new dark channel prior for removing haze from the image. Unlike the traditional dark-channel prior that assumes a zero minimal value, the new prior searches for the darkest pixel in each ellipsoid. Recently, Zhu et al. [16] proposed a new, simple and powerful prior-color attenuation prior based on statistics of natural images. A linear model for the scene depth of the fog image with the color attenuation prior was created to solve the model parameters via supervised learning. With the resulting depth map, the air-light can be easily recovered. Li et al. [17] proposed to decompose the simplified dark channel of the hazy image into a detail layer and a base layer based on edge-preserving decomposition. The base layer was used to estimate the transmission map for restoring the haze-free images.

To effectively remove haze from a single image, some methods based on the principle of image fusion have been proposed recently. Ancuti et al. [18,19] show the effectiveness of the fusion-based method for removing haze from a single input image. The fusion-based method proposed in [19] first pre-processed two original hazy image inputs by applying a contrast enhancing and a white balance procedure. Then it blended the resulting inputs by computing three measurements (weight maps). Furthermore, it adopted a multiscale strategy to reduce the artifacts. This method can produce good results similar to and even better than complex state-of-the-art techniques. In contrast, Wang et al. [20] used a multiscale depth fusion method to recover a haze-free image. A new technique was proposed to estimate the depth by considering the influence of noise. They developed an inhomogeneous Laplacian-Markov random field with edge-preserving and smooth constrains for multiscale depth fusion to estimate a depth map and produce an improving contrast and vivid color result.

In this paper, we propose to replace the widely used soft matting [2] and contextual regularization [21] in estimating the transmission map for haze removal by first finding some fixed points in a maximum filter and then applying a Nearest-Neighbor (NN) regularization. Figure 1 shows an illustrative example for our proposed dehazing method. Experimental results on some typical and challenged images illustrate that our method can produce a high-quality dehazed and vivid color image.

2   Background

2.1   Haze Imaging Model

In computer graphics and computer vision, the haze imaging model presented in [1], which describes the formation of a hazy image, is widely used as following:

$$\mathbf{I}(\mathbf{x}) = \mathbf{J}(\mathbf{x})t(\mathbf{x}) + A(1 - t(\mathbf{x})), \tag{1}$$

where $\mathbf{x}$ is a pixel location, $\mathbf{I}$ is the observed haze image, $\mathbf{J}$ is the haze free image, $\mathbf{I}(\mathbf{x})$ and $\mathbf{J}(\mathbf{x})$ stand for the intensities of the point $\mathbf{x}$ in $\mathbf{I}$ and $\mathbf{J}$, respectively, A is the air light (or atmospheric light) of the haze image, and t is the transmission coefficient, which describes the probability of the light reflecting from object is not scattered and absorbed by air particles. Recovering a haze free image $\mathbf{J}$ from the observed haze image $\mathbf{I}$ is equal to solve A and t from $\mathbf{I}$.

As we can see, the longer light traveling before reaching a camera, the more scattered and attenuated. Thus, we can express the transmission coefficient t as follows:

$$t(\mathbf{x}) = e^{-\beta d(\mathbf{x})}, \tag{2}$$

where $d(\mathbf{x})$ represents the distance between the camera and the scene point corresponding to $\mathbf{x}$, and β represents the attenuation coefficient of the atmosphere (often set to 1). So from Eq. (1), we find that the contribution of the air-light term A is more important when the observed scene is far away from the camera.

2.2   Nonlinear Filtering

Nonlinear filtering is often used to get a good bound transmission for each pixel. There are two kinds of filters: pixel-wise and patch-based. Nishino et al. [22], and Caraffa and Tarel [23] applied a pixel-wise nonlinear operation to recover a finer estimation of the transmission map, and then imposed a Markov regularization using the contextual constrain. The fine estimation prevents from the block artifacts and halos of the patch-based filter, but more constraints are needed to recover a high accurate transmission map. The white objects and the farther objects make it hard to estimate the transmission map accurately. He et al. [2] applies a patch-based filter to solve the white objects problem. While the patch-based filter can solve the white object problem, both block artifacts and halos incurred by the patch-based filter need to be further solved.

2.3   Fixed-Point Theorem

The fixed-point theorem [24] has been proposed for a long time. In mathematics, a fixed-point theorem is a result saying that a function F will have at least one fixed point (a point x for which $F(x) = x$), under some conditions on F that can be stated in general terms. In this paper, we define the point x as a fixed one if it satisfies the following equation:

$$F(x) = x. \tag{3}$$

2.4   Non-local Principle

Non-local principle has attracted a lot of attention for its broad applications, such as denoise [25] and matting [26,27]. As stated in [25], the nonlocal principle is that for a given distorted image, the pixel can be restored by taking a weighted sum of the pixels that have similar appearance, where the weights are given by a kernel. In our proposed single image dehazing approach, we apply the similar principle, but we make some modifications so as to better suit the regularization problem. These modifications will be described in details in Sect. 3.4.

3   Our Approach

3.1   Atmospheric Light Estimation

There exist a lot of methods to estimate the atmospheric light, i.e., the parameter A in Eq. (1). He et al. [2] proposed a method to estimate A based on the dark channel prior. Kim et al. [28] also proposed an approach based on the quadtree based subdivision, which may be more suitable for our application because the method proposed by He et al. [2] is based on the dark channel prior, which is not required in our proposed method. However, we still adopt He et al.'s method because of its efficiency. We first compute the dark channel prior of a hazy image. Second we pick up the top 0.1% of the dark channels. Third we

find out the pixel with highest intensity as the atmospheric light. According to Eq. (2), when the objects are far away from the camera, the depth is very large and the transmission of the objects is close to 0. According to the haze imaging model in Eq. (1), when the transmission is equal to 0, the observed object intensity in the hazy image is equal to the atmospheric light, i.e.,

$$\mathbf{I}(\mathbf{x}) = \mathbf{J}(\mathbf{x})t(\mathbf{x}) + A(1 - t(\mathbf{x})) = A. \tag{4}$$

This method also works well when the image doesn't have pixels at infinite distance because t in most haze-opaque regions is very small and the influence of sunlight is so weak that can be ignored.

3.2   Lower Bound of Transmission

In order to get an initial transmission value of some pixel in an image, we rewrite Eq. (1) as following:

$$\mathbf{J}(\mathbf{x}) = \frac{\mathbf{I}(\mathbf{x}) - A(1 - t(\mathbf{x}))}{t(\mathbf{x})}. \tag{5}$$

In the RGB color space, the intensities of the image pixel fall in range $[0, 255]$. In order to facilitate the calculation, we normlize the intensities into range $[0, 1]$ correspondingly. In this way, we get the following equation:

$$0 \leq \frac{\mathbf{I}(\mathbf{x}) - A(1 - t(\mathbf{x}))}{t(\mathbf{x})} \leq 1, \tag{6}$$

which can result in the following two equations:

$$t_1(\mathbf{x}) \geq \frac{\mathbf{I}^c(\mathbf{x}) - A^c}{1 - A^c} \quad \text{and} \quad t_2(\mathbf{x}) \geq 1 - \frac{\mathbf{I}^c(\mathbf{x})}{A^c}, \tag{7}$$

where the superscript 'c' represents one of the RGB channels. The minimum transmission in the above two inequations are written as:

$$\hat{t}_1(\mathbf{x}) = \frac{\mathbf{I}^c(\mathbf{x}) - A^c}{1 - A^c} \quad \text{and} \quad \hat{t}_2(\mathbf{x}) = 1 - \frac{\mathbf{I}^c(\mathbf{x})}{A^c}. \tag{8}$$

Thus, the lower bound of the transmission can be defined as:

$$t_b(\mathbf{x}) = \max\left(\hat{t}_1(\mathbf{x}), \hat{t}_2(\mathbf{x})\right), \tag{9}$$

which is a special case of the lower bound of the transmission used in [21] with the parameters $C_0 = 0$ and $C_1 = 255$ as:

$$t_b(\mathbf{x}) = \min\left(\max\left(\frac{A^c - \mathbf{I}^c(\mathbf{x})}{A^c - C_0}, \frac{A^c - \mathbf{I}^c(\mathbf{x})}{A^c - C_1}\right), 1\right). \tag{10}$$

3.3   Fixed Points of Filtering

Nonlinear filtering is a popularly used operation to obtain the transmission map from the chromaticity of a hazy image. In our approach, we use the maximum-minimum filter as used in [21] to get a transmission as:

$$\tilde{t}(\mathbf{x}) = \min_{\mathbf{y} \in \Omega(\mathbf{x})} \max_{\mathbf{z} \in \Omega(\mathbf{y})} t(\mathbf{z}), \tag{11}$$

where $\Omega(\mathbf{x})$ and $\Omega(\mathbf{y})$ represent local patches centered at the points $\mathbf{x}$ and $\mathbf{y}$, respectively.

Based on the dark channel prior proposed by He et al. [2], we can estimate the transmission value of each pixel. Then, a rough transmission map can be recovered via the maximum-minimum filtering. To recover a more accurate transmission map, we first need to find the stable points whose transmission values are more accurate. The fixed-point theorem can be used to find such these stable points. For a given pixel $\mathbf{x}$ in a hazy image, if we apply the maximum-minimum filter on $\mathbf{x}$ with its lower bound transmission value $t_b(\mathbf{x})$, $\mathbf{x}$ is a fixed point if the following condition is satisfied:

$$F(t_b(\mathbf{x})) = t_b(\mathbf{x}), \tag{12}$$

where the function F stands for the maximum-minimum filter. Figure 2 shows an example of fixed points found with two different filter patch sizes, from which we can observe that the use of a smaller patch size will generate more fixed points.
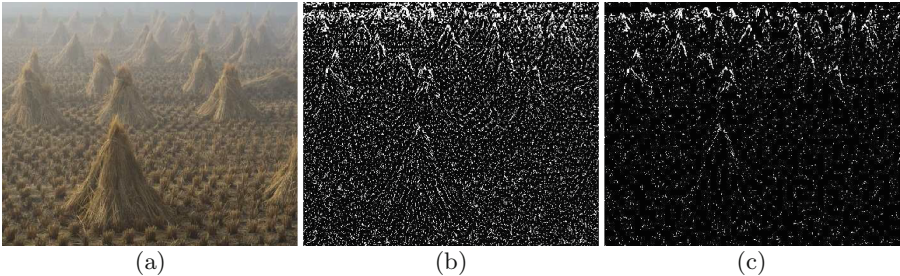

(a)   (b)   (c)

Fig. 2. An example of fixed points extracted from the input hazy image (a) with two different filter patch sizes, 7×7 (b) and 17×17 (c).

3.4   Nearest-Neighbor Regularization

Figure 3 shows two hazy images with their corresponding transmission maps, from which we can observe that the transmission map is very smooth except abrupt depth jumps. As mentioned before, the dehazing problem is severely under-constrained. Therefore, we need to introduce some assumptions on the natural transmission map. As stated before, the non-local principle considers a

Fig. 3. Hazy images in the left and their corresponding transmission maps in the right.

pixel as a liner combination of similar pixels in neighborhood. In the dehazing context, we consider an assumption that similar pixels have same transmission value. As stated in [9,21], our assumption is quite reasonable and widely used in most dehazing methods.

To efficiently measure the similarity between two image pixels, we need to consider the color similarity and spatial variation and smoothness. Given an image point $\mathbf{x}$, we define its feature vector for similarity measurement as follows:

$$f(\mathbf{x}) = (R, G, B, \lambda x, \lambda y)^\top, \tag{13}$$

where R, G and B represent the intensities of $\mathbf{x}$ in three RGB channels, respectively, x and y are the spatial coordinates of $\mathbf{x}$, and λ is balancing factor.

Although we use the same feature as in [27], but dehazing is different from matting, so for we need to modify the non-local principle widely used for matting.
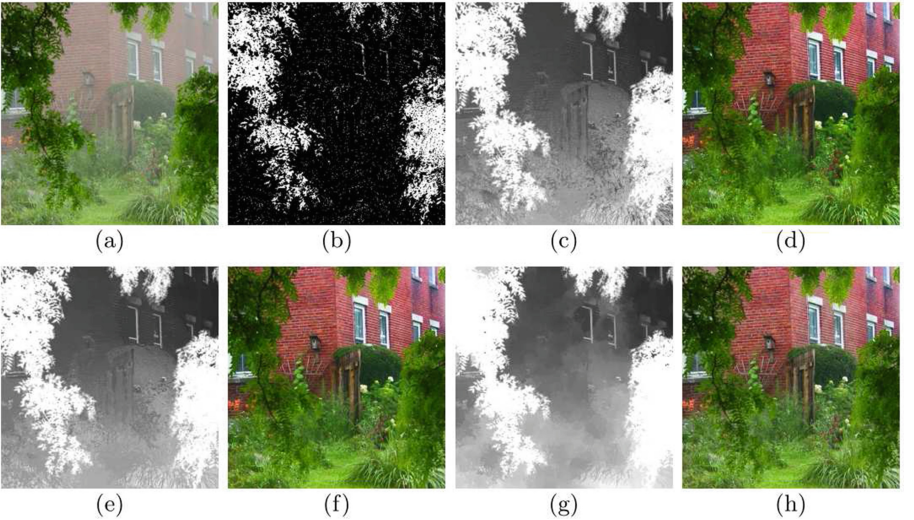

Fig. 4. The dehazing results with different values of λ: (a) the input hazy image; (b) fixed points; (c)–(d) the estimated transmission map and the dehazed image with $\lambda = 1$; (e)–(f) the estimated transmission map and the dehazed image with $\lambda = 2$; (g)–(h) the estimated transmission map and the dehazed image with $\lambda = 10$.
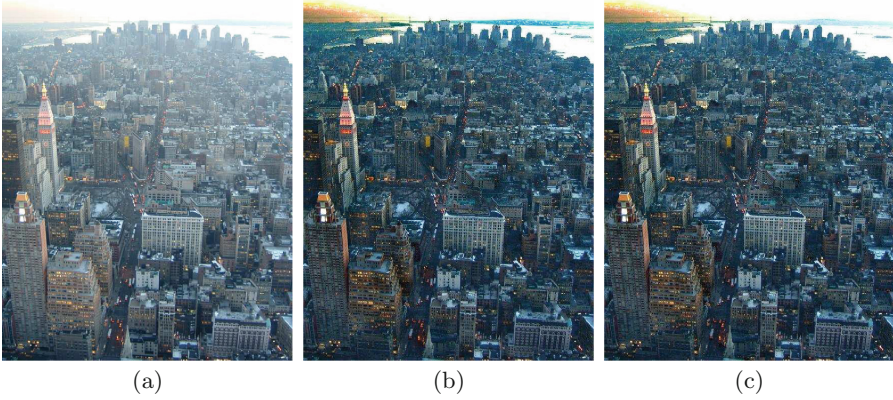
(a)   (b)   (c)

Fig. 5. The dehazed images with the use of the RGB (b) and HSV (c) color spaces from the input hazy image (a). (Color figure online)

In this paper, we treat the transmission values of fixed points as accuracy and reasonable, and we propose to recover the transmission values of the remaining points by finding their nearest neighbours from the set of fixed points based on the constructed k-d tree with the 5-dimensional feature vectors defined in Eq. (13). Given the atmospheric light A and the recovered transmission, a haze free image can be solved using the following equation:

$$\mathbf{J}(\mathbf{x}) = \frac{\mathbf{I}(\mathbf{x})) - A}{t(\mathbf{x})} + A. \tag{14}$$

Figure 4 shows the dehazing results with different values of the balancing factor λ, from which we can observe that the large value of λ will result in a more smooth transmission map, which is quite consistent with our assumption.

The HSV color space can be alternate of the RGB color space for similarity measurement. Figure 5 shows the dehazed images with the RGB and HSV color spaces, respectively, from which we observe that some hazy image regions cannot be clearly removed with the use of the HSV color space. By contrast, the RGB color space will produce a better dehazed image. So, the RGB color space is used in our method.

3.5   Our Dehazing Framework

The framework of our proposed single image dehazing method is summarized in Algorithm 1.

Algorithm 1. Our proposed single image dehazing framework.

Input: The hazy image.
Output: The haze free image.
 1: Compute the atmospheric light A using Meng et al.'method;
 2: Compute the lower bound of the transmission;
 3: Find the fixed points with the maximum-minimum filter;
 4: Recover the transmission map by the nearest neighbour (NN) regularization;
 5: Recover the haze free image using the atmospheric light A and the recovered transmission map.

---

4   Experimental Results

In order to evaluate the effectiveness of the proposed dehazing method, we tested it on a lot of hazy images and compared it with some state-of-the-art methods [2,5,7–9,12,19]. In all examples presented in this section, we assume the atmospheric light estimation is given by using the air-light vector A calculated by [21] or selecting the densest hazy pixel. All the results of other methods come from the Fattal's homepage[1].

4.1   Tests on Typical Examples

Figure 6 shows the dehazed result on an example image with inhomogeneous fog. Figure 7 shows the dehazed results on three example images with homogeneous fog. For these example images we used the patch size 17×17 and $\lambda = 2$. As we can see from Figs. 6 and 7, we can observe that our dehazed images present full details and vivid color information recovered from the fog or hazy images. As stated in [21], the fog in the image of "Tiananmen" cannot be regarded as homogeneous. This case often happens due to the large area of sky in the image. For this hazy image, we use the atmospheric light A selected by manual, the values were set as $[0.7961, 0.7529, 0.6588]$ for the RGB channels, respectively. We also draw the same conclusion with [21] that the transmission map represents the density of the hazes or fogs in the captured image.

4.2   Visual Comparison

We also compared our method with several state-of-the-art methods. Figure 8 illustrates an example with the comparisons between our method and the other two methods: He et al.'s [2] and Fattal's [9]. For this example, we used the parameters with $A = [0.53, 0.53, 0.53]$, the patch size 40×40, and $\lambda = 10$. The A value was used in the Fattal's work [9]. From Fig. 8, we can see that our method can restore the finer details and vivid color from the hazy regions.

Figure 9 shows the dehazed result using our method on a heavy hazy image by comparison with the other two recent methods. From Fig. 9, we can observe

---

[1] Available at http://www.cs.huji.ac.il/~raananf/projects/dehaze_cl/.

Fig. 6. The dehazed result on the "Tiananmen" image using our method: (Left) the input hazy image; (Middle) the recovered transmission map; (Right) the dehazed image. (Color figure online)
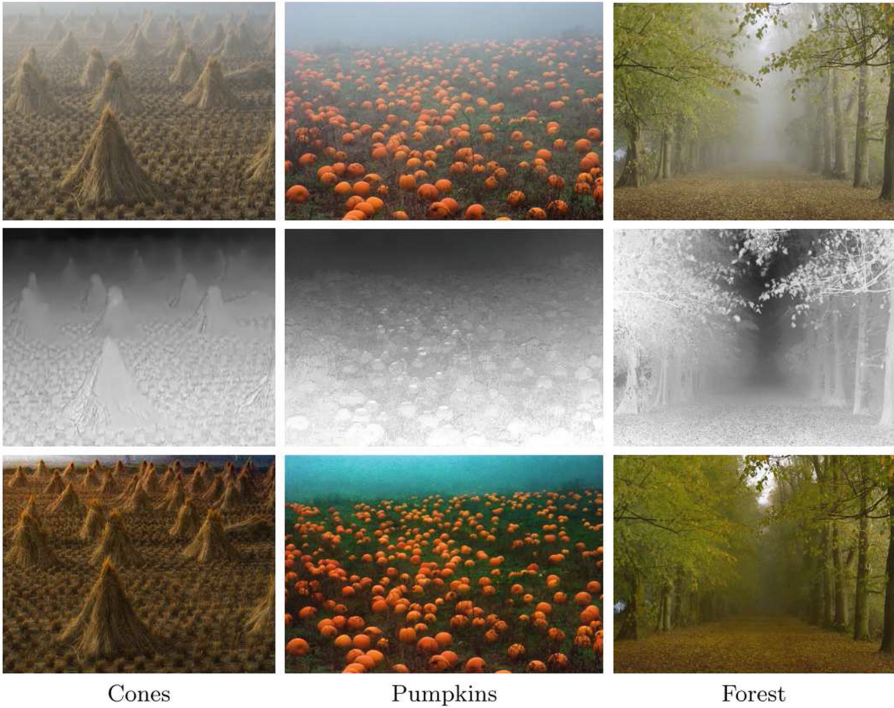

Cones   Pumpkins   Forest

Fig. 7. The dehazing results on three typical images: (Top) the input hazy images; (Middle) the recovered transmission maps; (Bottom) the dehazed images. (Color figure online)

that our result on this heavy hazy image is comparable in terms of visual quality to those results in [19,29]. For this example, we used the parameters with $A = [0.63, 0.62, 0.62]$, the patch size 40×40, and $\lambda = 10$. As we can see from Fig. 9, the Ancuti et al.'s method [19] and Choi et al.'s method [29] cannot remove the haze completely. In contrast, our method can restore the detail information and vivid color well.
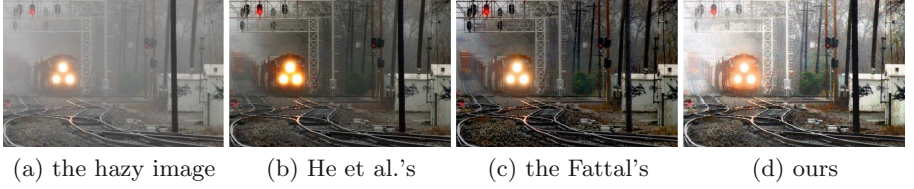
(a) the hazy image   (b) He et al.'s   (c) the Fattal's   (d) ours

Fig. 8. An illustrative comparison with the He et al.'s and the Fattal's methods. (Color figure online)

Input   Ancuti et al.'s   Choi et al.'s   Ours
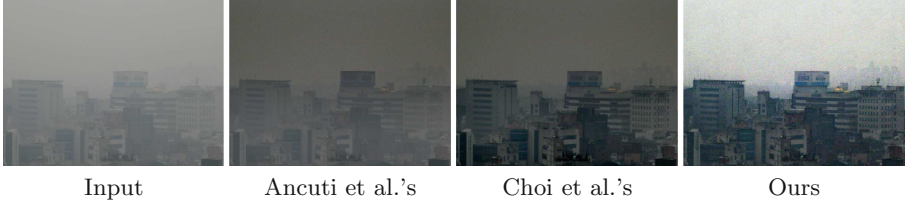
Fig. 9. An illustrative comparison with the Ancuti et al.'s and the Choi et al.'s methods.

Figures 10 and 11 show the comparison of our method with the other six state-of-the-art methods on "ny12" and "ny17" images, respectively, which are widely used for testing the performance of the dehazing method. Tan's method [7] can greatly enhance the image visibility and recover the image details. However, the colors in the restored images are often over enhanced. Since this method is not a physical sound and the transmission may thus be underestimated. Tarel et al.'s method [12] is a filtering based method. Its greatest advantage is real time while its dehazed images are not quite visual pleased. The Fattal's method [8] estimates the transmission based on the sufficient color information. When the haze is very heavy, the transmission may be wrongly estimated. He et al.'s method is a statistics based method, it can produce a very good result. But it may be fail in regions with many depth jumps. Ancuti et al.'s method is a fusion-based method and can produce a visually pleasing result. For the "ny17" image, in order to reduce the noise of the result image we restrict the transmission value between 0.2 and 1, and our result can recover a high quality and rich details from the hazy image. In order to equally compare the result, we used the value of A reported in [9].

4.3   Quantitative Comparison

Based on the above results on the "ny12" and "ny17" images, we conducted a quantitative comparison using the blind assessment of [30]. Hautière et al. [30] computed the ratio between the gradients of the input image and the restored one. This method is based on the concept of the visibility level, which is widely used in lighting areas. Table 1 shows the quantitative comparisons on the "ny12"

(a) "ny12" image   (b) Tan's   (c) Fattal'   (d) He et al.'s

(e) Kopf et al.'s   (f) Ancuti et al.'s   (g) Tarel et al.'s   (h) Ours

Fig. 10. Comparisons with the state-of-the-art methods on the "ny12" image.

(a) "ny12" image   (b) Tan's   (c) Fattal'   (d) He et al.'s

(e) Kopf et al.'s   (f) Ancuti et al.'s   (g) Tarel et al.'s   (h) Ours
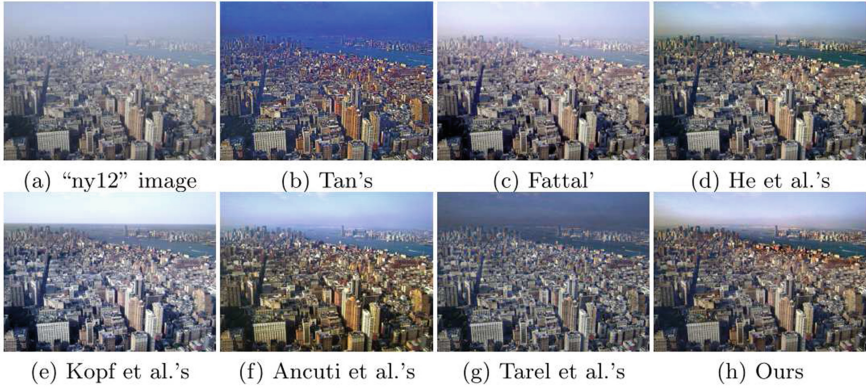
Fig. 11. Comparisons with the state-of-the-art methods on the "ny17" image.

and "ny17" images, in which the indicator "e" represents the newly visible edges ratio after restoration, the indicator "$\sum$" represents the percentage of pixels which are completely white or dark after restoration, and "$\bar{r}$" represents the mean ratio of the gradients at visible edges.

From Table 1, we can observe that all tested methods (including our method) produce a small value of the indicator $\bar{r}$, which represents the ratio of the pixels

Table 1. Quantitative comparison on the "ny12" and "ny17" images based on three indicators, e, $\sum$ and $\bar{r}$ used in [30].

Image	Tan's			Fattal's			Kopf et al.'s			He et al.'s		
	e	$\sum$	$\bar{r}$	e	$\sum$	$\bar{r}$	e	$\sum$	$\bar{r}$	e	$\sum$	$\bar{r}$
ny12	-0.14	0.02	2.34	-0.06	0.09	1.32	0.05	0.00	1.42	0.06	0.00	1.42
	Tarrel et al.'s			Ancuti et al.'s			Choi et al.'s			Ours		
	0.07	0.0	1.88	0.02	0.00	1.49	0.09	0.00	1.56	0.06	0.00	1.36
Image	Tan's			Fattal's			Kopf et al.'s			He et al.'s		
ny17	-0.06	0.01	2.22	-0.12	0.02	1.56	0.01	0.01	1.62	0.01	0.00	1.65
	Tarrel et al.'s			Ancuti et al.'s			Choi et al.'s			Ours		
	-0.01	0.0	1.87	0.12	0.00	1.54	0.03	0.00	1.49	0.14	0.00	1.82

being completely white or dark. On the one hand, the indicator e shows that most methods remove some of the visible edges, Only our method, He et al.'s [2] and Ancuti et al.'s [19] are positive values of the indicator e for these two test images. On the other hand, for the indicator $\sum$, the measurement [30] yields small values of the indicator $\sum$ for our results, which means our method doesn't have the problem of over-saturation. The values of our results are close to $\bar{r} = 1$, which show that the local contrast was restored moderately, He et al.'s [2], Kopf et al.'s [5] and Fattal's [8] methods also have this feature. In contrast, Tarel et al.'s [12] and Tan's [7] methods increase the local contrast too strongly and as a result these methods have a high values of the indicator $\bar{r}$. In general the method with low values of the indicator $\bar{r}$ show less artifacts and spurious. To the best of our knowledge, the blind assessment of [30] is the only method designed to produce a quantitative explanation for defogging operation. The indicators can give some explanations to the level of restoration and degradation, which can be used to measure the performance of the dehazing method.

5   Conclusion

Haze removal is an important task in image and video editing and results in a great challenge for computer vision. In this paper, we proposed a novel method to reduce the block artifacts and halos for single image dehazing. First, we proposed a simple method to estimate the transmission for some pixels based on the fixed-point theorem. Then we introduced a new regularization method based on the assumption that the transmission map varies smoothly. Experimental results on some typical and challenged images illustrate that our method can produce good results comparative to and even better than the more complex state-of-the-art methods.

References

1. Harald, K.: Theorie der horizontalen Sichtweite: Kontrast und Sichtweite, vol. 12. Keim & Nemnich, Munich (1924)
2. He, K., Sun, J., Tang, X.: Single image haze removal using dark channel prior. IEEE Trans. Pattern Anal. Mach. Intell. **33**, 2341–2353 (2011)
3. Narasimhan, S.G., Nayar, S.K.: Contrast restoration of weather degraded images. IEEE Trans. Pattern Anal. Mach. Intell. **25**, 713–724 (2003)
4. Shwartz, S., Namer, E., Schechner, Y.Y.: Blind haze separation. In: IEEE Computer Society Conference on Computer Vision and Pattern Recognition (CVPR), vol. 2, pp. 1984–1991 (2006)
5. Kopf, J., Neubert, B., Chen, B., Cohen, M., Cohen-Or, D., Deussen, O., Uyttendaele, M., Lischinski, D.: Deep photo: model-based photograph enhancement and viewing. ACM Trans. Graph. (TOG) **27**, 32–39 (2008)
6. Schechner, Y.Y., Narasimhan, S.G., Nayar, S.K.: Instant dehazing of images using polarization. In: IEEE Computer Society Conference on Computer Vision and Pattern Recognition (CVPR), vol. 1, pp. 325–332 (2001)
7. Tan, R.T.: Visibility in bad weather from a single image. In: IEEE Computer Society Conference on Computer Vision and Pattern Recognition (CVPR), pp. 1–8 (2008)
8. Fattal, R.: Single image dehazing. ACM Trans. Graph. (TOG) **27**, 1–9 (2008)
9. Fattal, R.: Dehazing using color-lines. ACM Trans. Graph. (TOG) **34**, 13 (2014)
10. Chavez, P.S.: An improved dark-object subtraction technique for atmospheric scattering correction of multispectral data. Remote Sens. Environ. **24**, 459–479 (1988)
11. He, K., Sun, J., Tang, X.: Guided image filtering. IEEE Trans. Pattern Anal. Mach. Intell. **35**, 1397–1409 (2013)
12. Tarel, J.P., Hautiere, N.: Fast visibility restoration from a single color or gray level image. In: IEEE International Conference on Computer Vision (ICCV), pp. 2201–2208 (2009)
13. Tarel, J.P., Hautière, N., Caraffa, L., Cord, A., Halmaoui, H., Gruyer, D.: Vision enhancement in homogeneous and heterogeneous fog. IEEE Intell. Transp. Syst. Mag. **4**, 6–20 (2012)
14. Carr, P., Hartley, R.: Improved single image dehazing using geometry. In: Digital Image Computing: Techniques and Applications (DICTA), pp. 103–110 (2009)
15. Gibson, K.B., Nguyen, T.Q.: An analysis of single image defogging methods using a color ellipsoid framework. EURASIP J. Image Video Process. **2013**, 1–14 (2013)
16. Zhu, Q., Mai, J., Shao, L.: A fast single image haze removal algorithm using color attenuation prior. IEEE Trans. Image Process. **24**, 3522–3533 (2015)
17. Li, Z., Zheng, J.: Edge-preserving decomposition-based single image haze removal. IEEE Trans. Image Process. **24**, 5432–5441 (2015)
18. Ancuti, C.O., Ancuti, C., Hermans, C., Bekaert, P.: A fast semi-inverse approach to detect and remove the haze from a single image. In: Kimmel, R., Klette, R., Sugimoto, A. (eds.) ACCV 2010. LNCS, vol. 6493, pp. 501–514. Springer, Heidelberg (2011). doi:10.1007/978-3-642-19309-5_39
19. Ancuti, C.O., Ancuti, C.: Single image dehazing by multi-scale fusion. IEEE Trans. Image Process. **22**, 3271–3282 (2013)

20. Wang, Y., Fan, C.: Single image defogging by multiscale depth fusion. IEEE Trans. Image Process. **23**, 4826–4837 (2014)
21. Meng, G., Wang, Y., Duan, J., Xiang, S., Pan, C.: Efficient image dehazing with boundary constraint and contextual regularization. In: IEEE International Conference on Computer Vision (ICCV), pp. 617–624 (2013)
22. Nishino, K., Kratz, L., Lombardi, S.: Bayesian defogging. Int. J. Comput. Vis. **98**, 263–278 (2012)
23. Caraffa, L., Tarel, J.P.: Markov random field model for single image defogging. In: IEEE Intelligent Vehicles Symposium (IV), pp. 994–999 (2013)
24. Kakutani, S.: A generalization of Brouwer's fixed point theorem. Duke University Press, Durham (1941)
25. Buades, A., Coll, B., Morel, J.M.: A non-local algorithm for image denoising. In: IEEE Computer Society Conference on Computer Vision and Pattern Recognition (CVPR), vol. 2, pp. 60–65 (2005)
26. Lee, P., Wu, Y.: Nonlocal matting. In: IEEE Conference on Computer Vision and Pattern Recognition (CVPR), pp. 2193–2200 (2011)
27. Chen, Q., Li, D., Tang, C.K.: KNN matting. IEEE Trans. Pattern Anal. Mach. Intell. **35**, 2175–2188 (2013)
28. Kim, J.H., Jang, W.D., Sim, J.Y., Kim, C.S.: Optimized contrast enhancement for real-time image and video dehazing. J. Vis. Commun. Image Represent. **24**, 410–425 (2013)
29. Choi, L.K., You, J., Bovik, A.C.: Referenceless prediction of perceptual fog density and perceptual image defogging. IEEE Trans. Image Process. **24**, 3888–3901 (2015)
30. Hautière, N., Tarel, J.P., Aubert, D., Dumont, E.: Blind contrast enhancement assessment by gradient ratioing at visible edges. Image Anal. Stereology **27**, 87–95 (2008)

Springer